Electronic Supplementary Material (ESI) for Physical Chemistry Chemical Physics.

Supplementary Material for: Effects of Surfactant Adsorption on the Wettability and Friction of Biomimetic Surfaces

Erik Weiand[a,b,c,*], James P. Ewen[a,b,c,*], Yuri Roiter[d], Peter H. Koenig[d], Francisco Rodriguez-Ropero[d], Stefano Angioletti-Uberti[b,c,e], and Daniele Dini[a,b,c]

[a]Department of Mechanical Engineering, Imperial College London, South Kensington Campus, SW7 2AZ London, U.K.
[b]Institute of Molecular Science and Engineering, Imperial College London, South Kensington Campus, SW7 2AZ London, U.K.
[c]Thomas Young Centre for the Theory and Simulation of Materials, Imperial College London, South Kensington Campus, SW7 2AZ London, U.K.
[d]Corporate Functions Analytical and Data & Modeling Sciences, Mason Business Center, The Procter and Gamble Company, Mason, 45040 Ohio, U.S.A.
[e]Department of Materials, Imperial College London, South Kensington Campus, SW7 2AZ London, U.K.
[*]E-mails: erik.weiand19@imperial.ac.uk; j.ewen@imperial.ac.uk

1 Micelle aggregation numbers

Table S1 Aggregation numbers of surfactant micelles as a function of the bulk concentration in charge-neutral systems without excess salt.

a) CTAB		b) SDS	
c [mM]	$\overline{N}_{\mathrm{agg}}$ [-]	c [mM]	$\overline{N}_{\mathrm{agg}}$ [-]
139	7.1	174	8.1
278	11.6	312	12.5
368	20.0	447	15.9
484	23.9	563	22.1
579	28.9	664	21.5

2 Adsorption dependence on micelle aggregation number

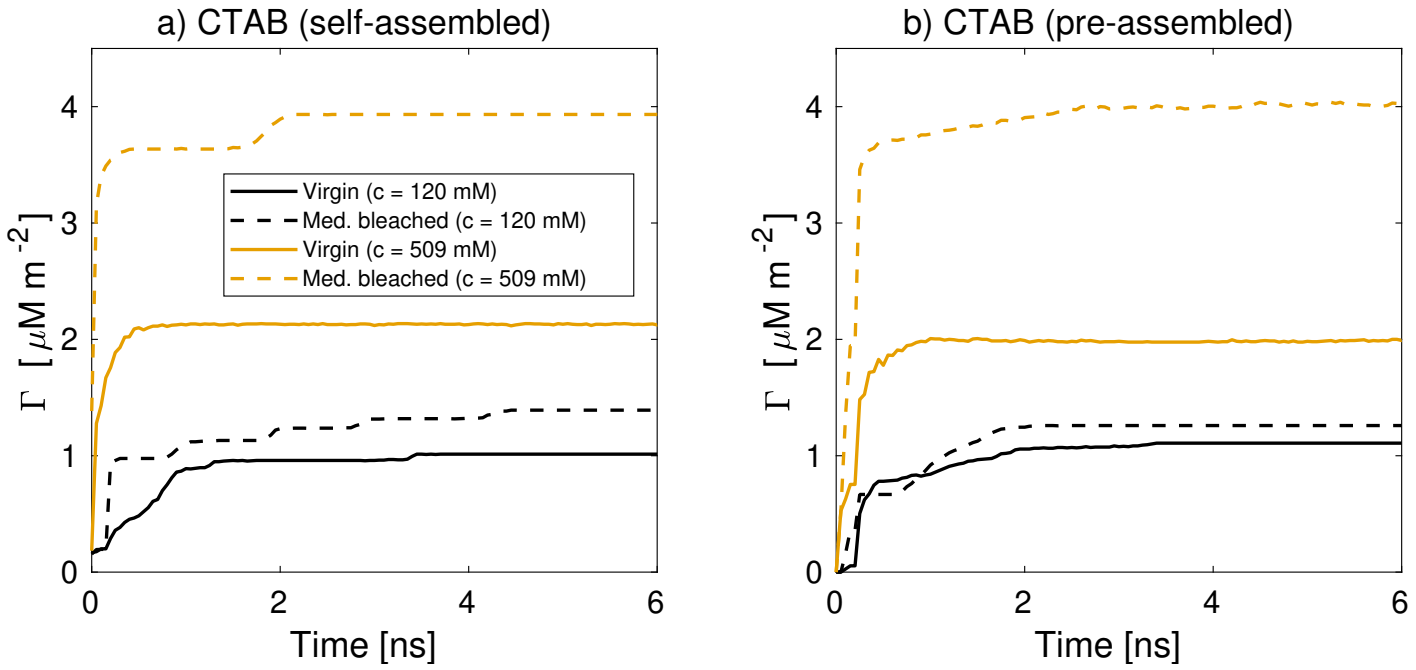

Figure S1 Temporal evolution of micelle adsorption to hair surfaces for a) self-assembled ($\overline{N}_{\mathrm{ag}} = 7.1 - 28.9$) and b) pre-assembled CTAB micelles ($\overline{N}_{\mathrm{ag}} = 82$). The agreement in adsorption kinetics and equilibrium adsorption densities suggests that adsorption is not sensitive the size nor stability of the micellar aggregates in bulk - likely because complete micelle break-up occurs near the surface due to electrostatic interactions with the anionic surface sites.

3 Initial counterion distribution

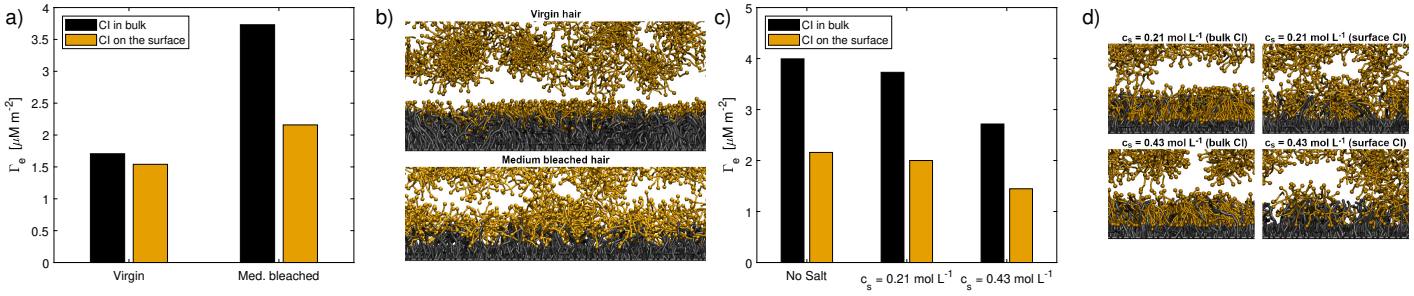

Figure S2 CTAB adsorption densities for initial counterion distributions either fully in the bulk or fully adsorbed on the surface. a) Difference between different degrees of surface damage with b) snapshots of the interface for virgin (top) and medium bleached (bottom) model hair surfaces when all counterions are initially located on the surface. c) Adsorption densities on medium bleached hair surfaces for different levels of background salt with d) corresponding snapshots of the interface. The CTAB concentration is $c_0 \approx 500$ mM for all shown cases. Salt ions are not shown for clarity.

Previous all-atom simulations of CTAB adsorption on mica surfaces suggest a strong dependency of the presence of a potassium (K^+) layer on the substrate.[1] Upon removal of this ionic layer, the conformation of adsorbed CTAB at equilibrium changed from a micellar structure towards a bilayer conformation. We conducted additional simulations to compare the configurations with all counterions initially distributed in the liquid phase to configurations where counterions were initially adsorbed to the negative surface charges on the hair surface (locally charge neutral). Fig. S2a)-b) shows the adsorption densities Γ and snapshots of adsorbed surfactant structures on surfaces representative of

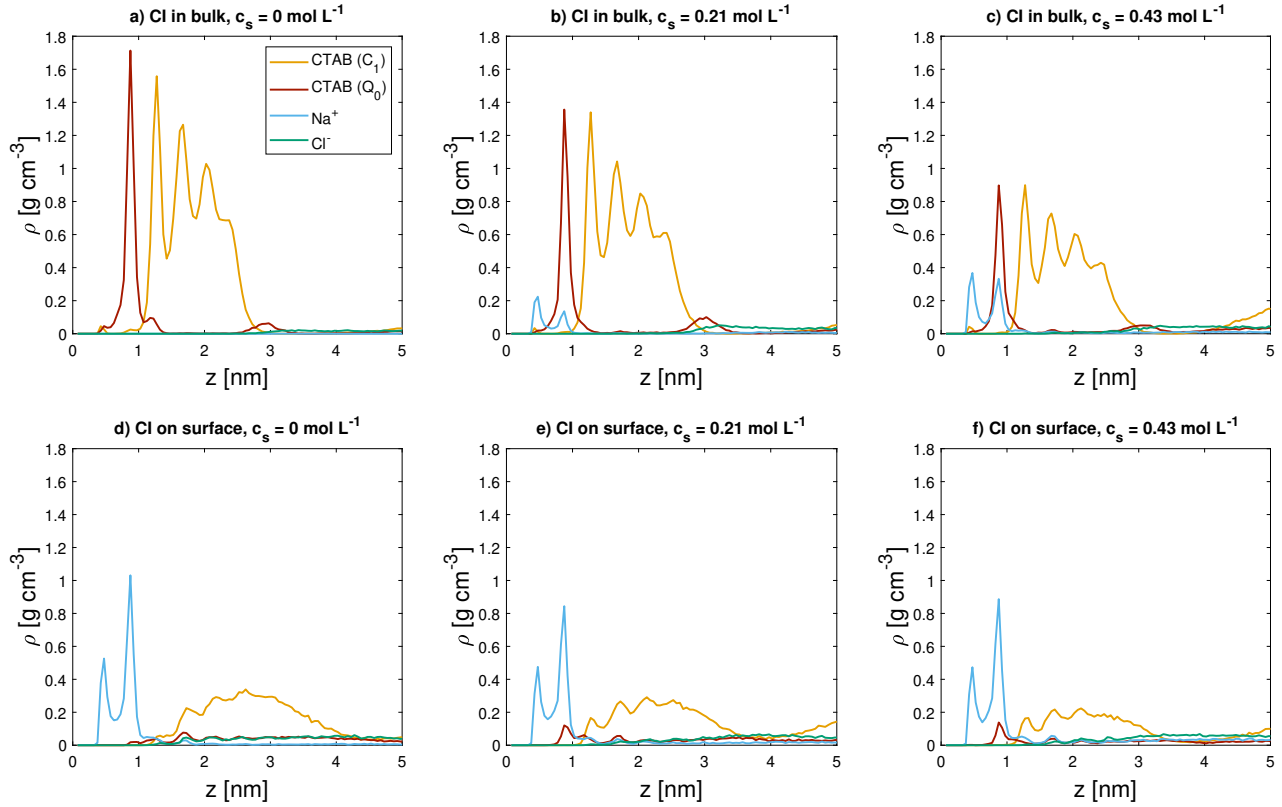

Figure S3 Density profiles of surfactants (CTAB) and ions at the medium bleached hair surface for initial counterion (Cl) distributions on either the surface or in the bulk. Three levels of excess salt concentrations are considered.

virgin and medium-bleached hair. For virgin hair, the adsorption density and corresponding ordered structure of CTAB on the surface do not change significantly between the two counterion configurations. For the strongly negatively charged surfaces representative of moderately bleached hair, we find that an initial distribution of neutralizing counterions on the surface leads to a decreased adsorption density of CTAB on the surface. The structure of adsorbed CTAB also becomes significantly more disordered as the surfactants appear to adsorb as micelles, which is consistent with Ref.[1] The corresponding equilibrium density profiles for the two extreme initial counterion configurations on bleached hair are shown in Fig. S3. In agreement with the snapshots in Fig. S2b), we find that the configuration of counterions (CI) initially on the surface indeed leads to a more disordered distribution of CTAB, as indicated by the density profiles of the cationic headgroup (Q_0). The counterions remain in their initial surface-adsorbed state during the adsorption simulations, thus reducing the absolute electrostatic surface potential. The electrostatic attraction thus becomes insufficient to break up the cationic surfactant micelles in the bulk, which explains the reduced adsorption density and more disordered nature of the adsorbed surfactant layer.

The coexistence of two adsorption states from different initial ion distributions indicates that at least one of these states should be metastable. In the case where all counterions are initially adsorbed, a transition to the first state could only be obtained by releasing counterions from the negatively charged surface sites. This mechanism is not observed at the timescales accessible in our simulations but might only be observed at significantly larger timescales. We conducted additional simulations for the two initial counterion distributions with an increased background ionic strength. Fig. S2c)-d) show the adsorption density and surface structure on bleached hair at long runtimes. The corresponding density profiles near the surface are shown in Fig. S3.

4 SDS adsorption contributions

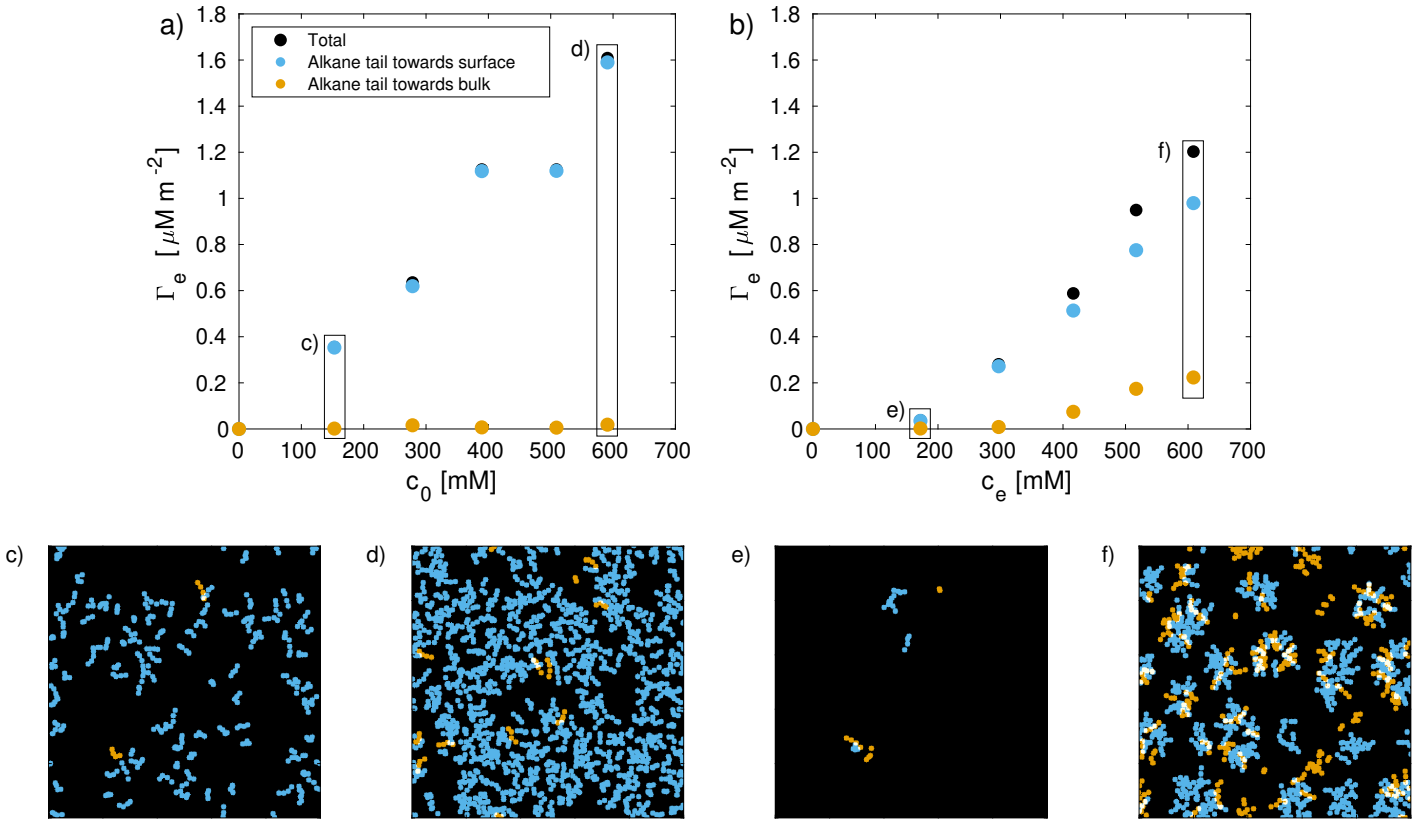

Figure S4 Top row: SDS adsorption densities for a) virgin and b) medium bleached model hair surfaces. The fraction of surfactants that adsorb with the alkane tail towards the surface (hydrophobic adsorption) and facing towards the bulk is shown for reference. Bottom row: Examples of instantaneous coverage fractions, modeling coarse-grained beads as planar disks with $r = \sigma_{\mathrm{LJ}}$. Regions of overlap are colored in beige. 18-MEA lipids are not shown for clarity. No fitting to a Langmuir model was attempted for SDS, as saturation is not observed on either of the two components nor on the total adsorption isotherm.

5 SDS sliding simulations

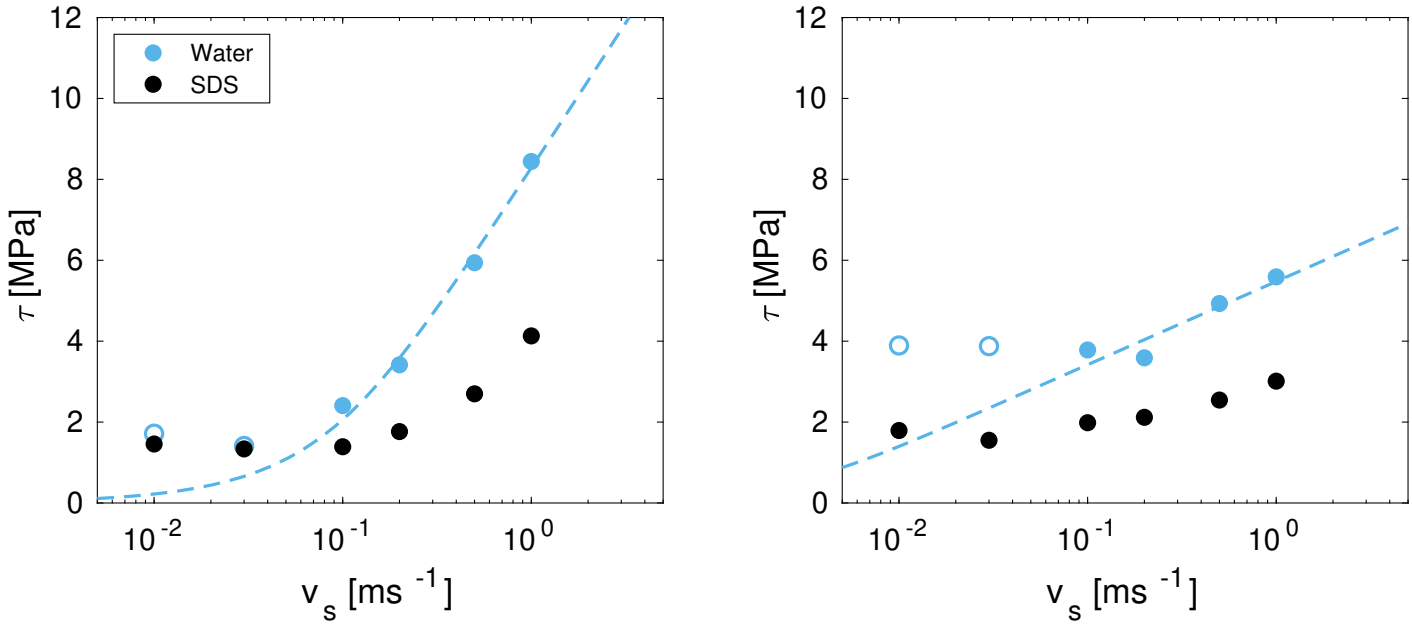

Figure S5 Shear stress between hair surfaces with water and SDS at 10 MPa on a) virgin hair ($\rho_{\mathrm{SDS}} = 0.28$ nm^{-2} after squeeze-out) and b) bleached hair ($\rho_{\mathrm{SDS}} = 0.98$ nm^{-2} after squeeze-out). A comparison to pure water contacts is provided with corresponding SATA fits according to Ref.[2].

6 Squeeze-out simulation contact composition

Table S2 CG water surface densities in the contact at the end of the squeeze-out simulations with pre-adsorbed CTAB as a function of normal pressure σ, hair damage and CTAB adsorption density Γ. Corresponding values for pure water hair contacts are reported in Ref.[2]

	a) Virgin hair		b) Med. bleached hair	
σ [MPa]	ρ_w ($\Gamma = 1.1$ μMm^{-2}) [nm^{-2}]	ρ_w ($\Gamma = 2.0$ μMm^{-2}) [nm^{-2}]	ρ_w ($\Gamma = 2.3$ μMm^{-2}) [nm^{-2}]	ρ_w ($\Gamma = 4.0$ μMm^{-2}) [nm^{-2}]
10	2.65	3.73	8.06	5.42
20	5.95	4.40	8.07	5.85
35	4.99	3.74	6.38	4.13
50	5.38	3.71	5.56	4.47

7 Combined lipid mass density profiles during NEMD simulations

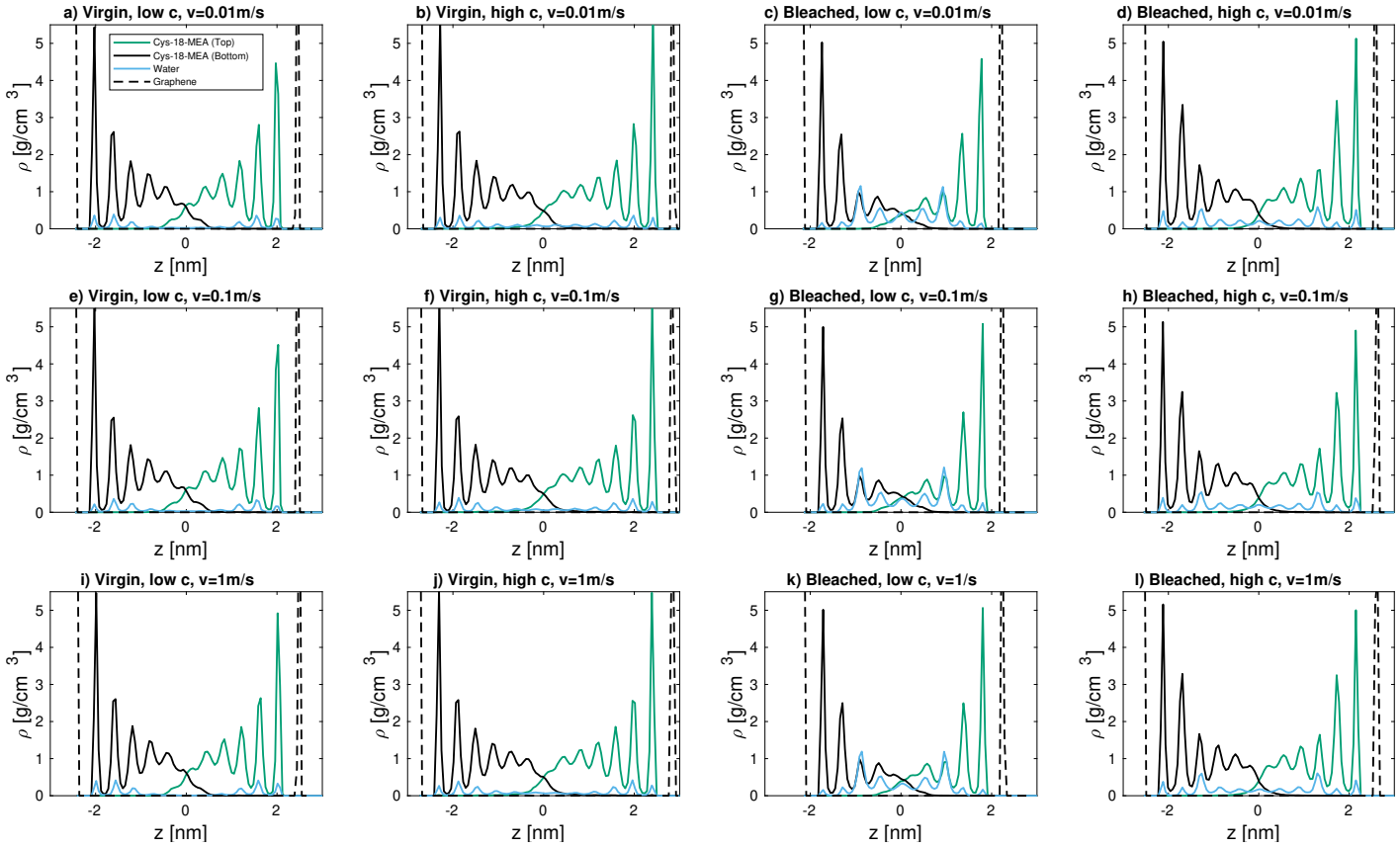

Figure S6 Mass density profiles for water and for lipids - comprised of both Cys-18-MEA and cationic surfactants (CTAB), i.e., $\rho = \rho_{\mathrm{MEA}} + \rho_{\mathrm{CTAB}}$ during sliding simulations for various v_s, degrees of hair damage χ and CTAB coverage Γ.

8 CTAB re-orientation during sliding

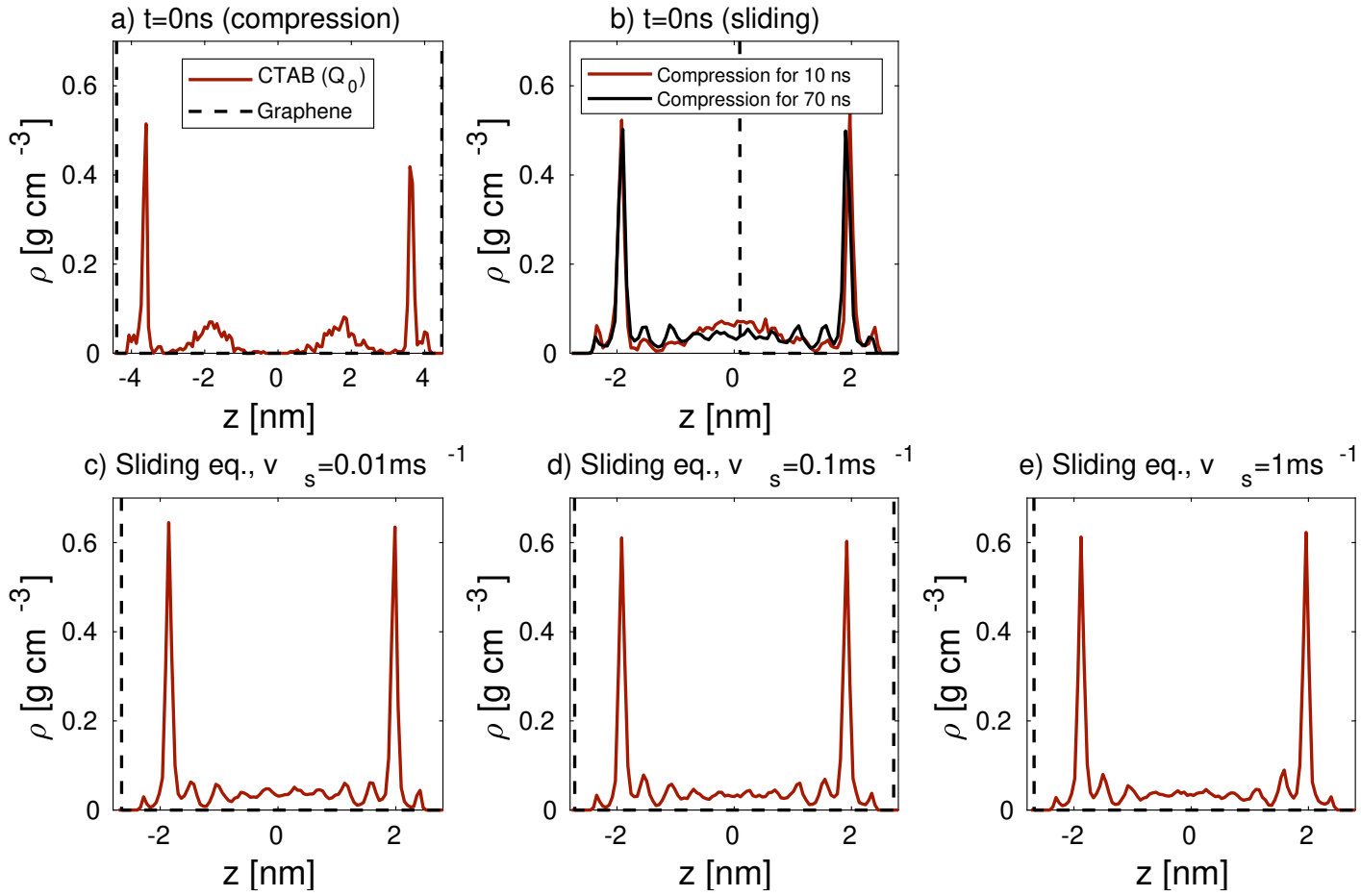

Figure S7 Mass density profiles for the Q_0 headgroup of cationic surfactants (CTAB) a) before compression, b) after compression for 10 ns and 70 ns, and c)-e) during sliding simulations (at dynamic equilibrium) for various v_s on virgin hair at $\Gamma_{\mathrm{CTAB}} = 2.0\ \mu\mathrm{Mm}^{-2}$, where the bilayer contribution is most prominent at the end of the adsorption simulations.

9 Surface charge separation

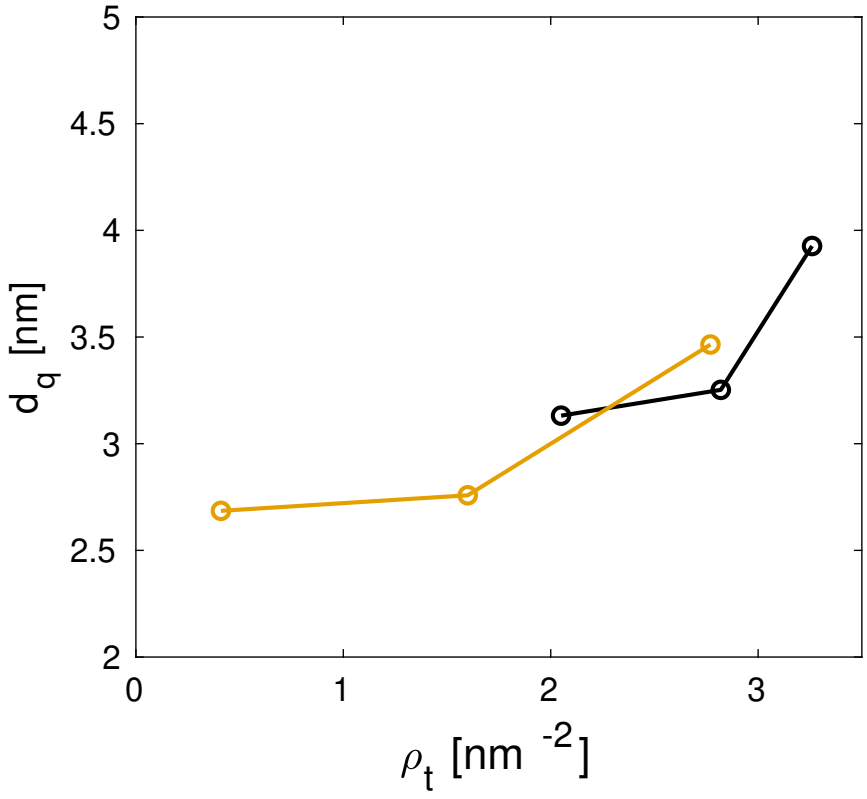

Figure S8 Distance between the charged cysteic acid groups on the two opposing surfaces for virgin (black) and bleached (orange) model hair surfaces.

10 CTAB mobility during sliding

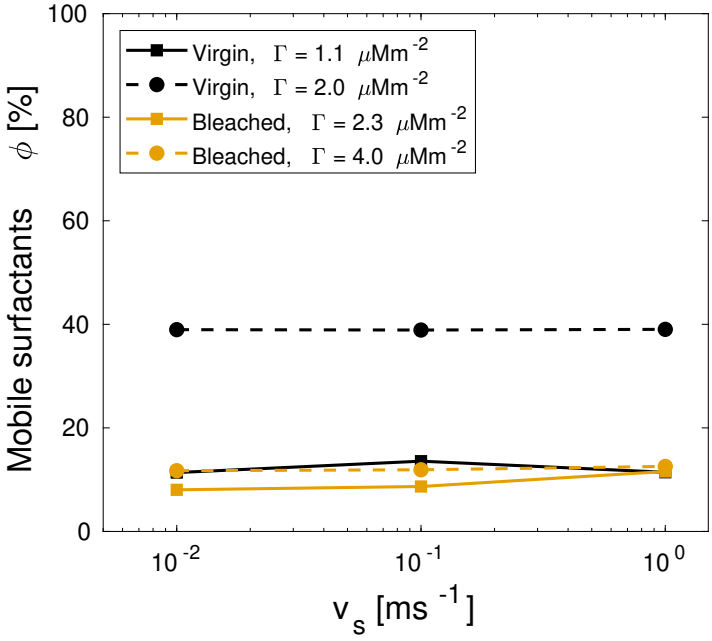

Figure S9 Mobility fraction[3] of cationic sites on CTAB for virgin and medium bleached hair surfaces at various degrees of surfactant coverage during sliding. CTAB molecules are considered to be desorbed if their cationic head group (Q_0) is located outside of a threshold ($d_a = 1.2$ nm) from the graphene sheet of each surface. The distance d_a is chosen to coincides with the first minimum after the primary adsorption peaks in the charge density profiles.

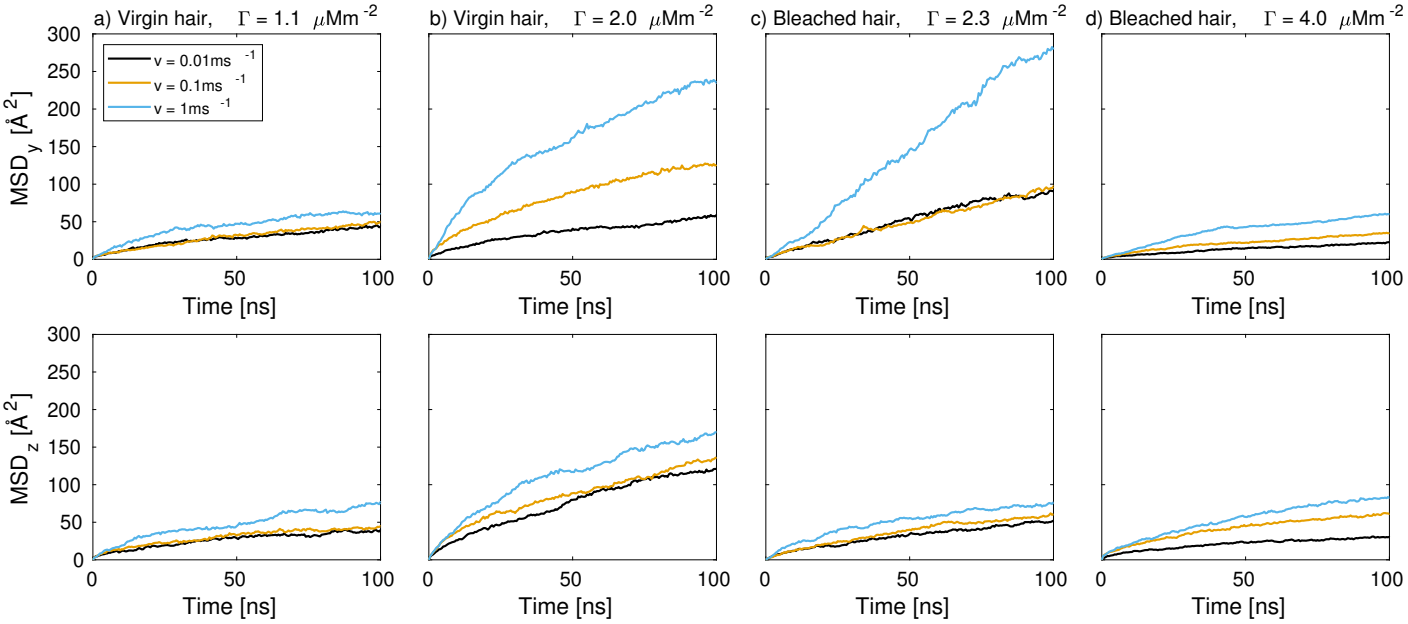

Figure S10 Mean-square-displacement in the y direction (MSD_y) and z direction (MSD_z) of cationic sites on CTAB for virgin and medium bleached hair surfaces at various degrees of surfactant coverage during sliding.

11 CTAB nematic order

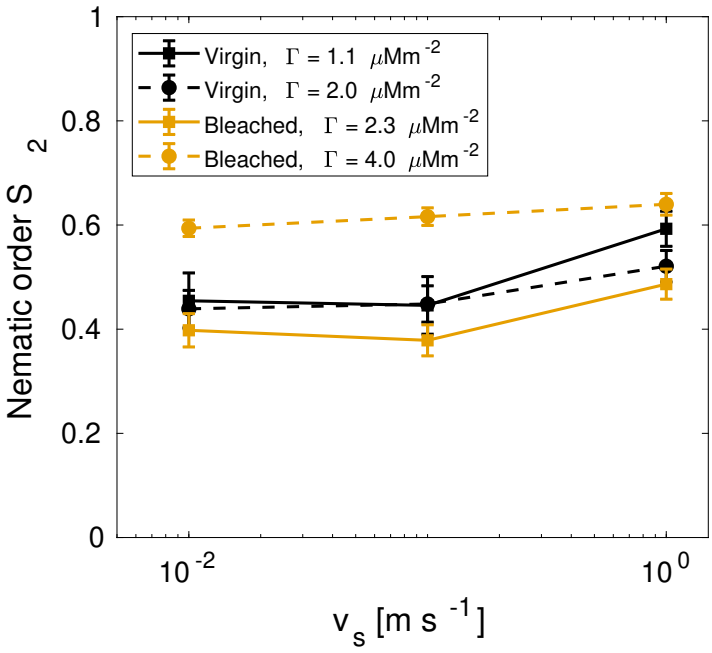

Figure S11 Nematic order[3] of cationic sites on CTAB for virgin and medium bleached hair surfaces at various degrees of surfactant coverage during sliding.

References

[1] G. Tsagkaropoulou, F. J. Allen, S. M. Clarke and P. J. Camp, *Soft Matter*, 2019, **15**, 8402–8411.

[2] E. Weiand, J. P. Ewen, Y. Roiter, P. H. Koenig, S. H. Page, F. Rodriguez-Ropero, S. Angioletti-Uberti and D. Dini, *Nanoscale*, 2023, **15**, 7086–7104.

[3] A. Z. Summers, C. R. Iacovella, M. R. Billingsley, S. T. Arnold, P. T. Cummings and C. McCabe, *Langmuir*, 2016, **32**, 2348–2359.